Received: 29 November 2024 | Revised: 7 February 2025 | Accepted: 16 February 2025
DOI: 10.1002/ppp3.70011

RESEARCH ARTICLE

Plants People Planet PPP Open Access

Sharing the light, impact of solar parks on plant productivity, soil microbes and soil organic matter

Luuk Scholten[1] | Ron G. M. de Goede[1] | Anna Edlinger[2] | Bas B. Van Aken[3] | Gerlinde B. De Deyn[1]

[1]Soil Biology Group, Wageningen University and Research, The Netherlands

[2]Wageningen Environmental Research, Wageningen University and Research, The Netherlands

[3]Solar Energy – TNO Energy & Materials Transition, Petten, The Netherlands

Correspondence
Luuk Scholten, Soil Biology Group, Wageningen University and Research, The Netherlands.
Email: luuk.scholten@wur.nl

Funding information
Rijksdienst voor Ondernemend Nederland, Grant/Award Number: MOOI-22004

Societal Impact Statement

Solar parks enable renewable energy production at a large scale, thereby reducing greenhouse gas emissions. However, the effects of this change in land use on vegetation and soil health are still largely unknown. In this study, we determined the impacts of solar parks on vegetation, soil biota and soil carbon between and below solar panels. We found lower plant and microbial biomass below the panels, while no differences in soil carbon pools were observed. The results stress the urgent need to design future solar parks that prevent soil degradation while still producing the renewable energy needed to combat climate change.

Summary

- Solar parks, large-scale arrays of photovoltaic panels, are a unique land use and play an important role in the renewable energy transition. However, the solar panels create shade and change the microclimate, potentially affecting plant growth and carbon inputs to the soil. These changes can influence key soil properties critical to long-term carbon storage and overall soil health. This study investigated the impact of commercial solar parks on plant productivity and the colonisation of roots by mycorrhizal fungi, soil organic matter (SOM), soil microbial community biomass and composition and litter decomposition in 17 solar parks with contrasting shading levels across the Netherlands.
- Soil samples and plant biomass samples were collected between and below the solar panels. The microclimate (temperature, moisture) was measured continuously over the growing season and cumulative solar irradiation during the growing season in relation to the solar panels was modelled.
- Results show that above- and below-ground plant biomass as well as mycorrhizal colonisation were significantly lower below than between panels, while we did not find differences for SOM, carbon stocks and hot water extractable carbon. Plant productivity related negatively to the extent of light interception by the panels. Furthermore, fungal and bacterial biomass and the F:B ratio were lower below compared to between the panels while decomposition rates did not differ.

- The severe decrease of plant biomass inputs in combination with maintained rates of decomposition are expected to result in decreased SOM stocks and soil health over time and suggest the need for guidelines for ecologically sound solar park designs to prevent soil damage.

KEYWORDS
microbial biomass, microclimate, plant–soil interactions, renewable energy, soil carbon storage, soil health, solar parks

1 | INTRODUCTION

To stabilise human-induced global warming, anthropogenic greenhouse gas emissions must be reduced to zero (Masson-Delmotte et al., 2021). Renewable energy sources, such as solar and wind energy, are key in reaching this goal by replacing fossil-based energy sources (Hernandez et al., 2014, 2019). Solar energy, currently the fastest growing renewable energy source (Bennun et al., 2021), is harnessed using photovoltaic modules, or solar panels, which can be installed on ground-mounted arrays to form a 'solar park'.

By the end of 2022, 562 solar parks had been installed in The Netherlands, covering a total area of 3,621 ha, often on former agricultural land (Bugera & Tillema, 2023; van Hooff et al., 2019). This transition from arable land or production grassland to solar parks likely impacts the local environment and its (soil) ecosystem services (Carvalho et al., 2023). Solar parks may increase local biodiversity if managed well, for example by establishing native flower-rich vegetation (Carvalho et al., 2023). However, by reducing plant-available solar radiation and by changing the microclimate (Armstrong et al., 2014), solar panels may hamper plant growth below the panels, thereby reducing carbon inputs to the soil, which may ultimately result in a decrease in soil organic matter (SOM; see Table S1 for a full list of abbreviations) content and soil health. SOM consists of approximately 50% of carbon and is central to soil health as it supports numerous soil-based ecosystem services, such as nutrient cycling, water retention, primary productivity and soil biodiversity (Adhikari & Hartemink, 2016; Bünemann et al., 2018; Creamer et al., 2022; Hoffland et al., 2020).

The effects of shading on plant growth vary depending on shade intensity and plant species (Poorter et al., 2019; Valladares et al., 2016; Valladares & Niinemets, 2008). While extreme shading (90%) can severely reduce vegetation growth (Abraham et al., 2014; Pierson et al., 1990; Semchenko et al., 2012), temperate grassland plants have been shown to still grow well under moderate shading conditions (50–75%) (Pang et al., 2019; Semchenko et al., 2012). Nevertheless, studies on vegetation responses to the presence of solar panels show contrasting results, with increases (Adeh et al., 2018) and major decreases (Armstrong et al., 2016) in plant biomass production below the panels. These variable vegetation responses in solar parks may be due to the context in which the shading occurs, and solar panel-induced alterations in other environmental factors apart from shading.

Besides shading, solar panels can alter microclimatic conditions, such as changes in (soil) temperature and moisture conditions beneath and between the panels. These changed microclimatic conditions can in turn affect plant growth as well as the activity of soil biota, the functions they provide and the soil carbon balance. Earlier research in solar parks showed that air and soil temperature beneath panels is lower compared to open areas, with larger differences during the growing season and daytime and no or small differences during winter and at night (Armstrong et al., 2016; Makaronidou, 2020; Yue et al., 2021). Solar parks may also change soil moisture and the spatial distribution of water. Interception of precipitation by panels reduces precipitation reaching the soil below the panels, potentially causing drier conditions; whereas reduced temperatures and vegetation growth beneath panels may also reduce evapotranspiration, conserving soil moisture (Armstrong et al., 2014; Yue et al., 2021). Furthermore, the intercepted rainfall often concentrates at the lower edge of interconnected panels (Armstrong et al., 2014; Choi et al., 2020; Yue et al., 2021), or between individual panels when gaps are present, leading to 'drip lines' on the soil surface, inducing spatial heterogeneity and gradients in soil properties between areas beneath, near and in between the panels (Makaronidou, 2020). This spatial heterogeneity in the microclimate could increase biodiversity within sites by increasing the number of microsites or buffer against climate extremes such as heatwaves and droughts (Sturchio & Knapp, 2023).

By altering plant growth and microclimate, solar parks may also change SOM levels and their spatial distribution, creating differences beneath and between panels. SOM stocks are the result of the balance between organic matter inputs and decomposition. Plant-derived carbon, fixed through photosynthesis, is the predominant source of carbon input into the soil (Janzen et al., 2022; Wiesmeier et al., 2019), and is essential for maintaining or increasing SOM stocks. SOM decomposition, driven by the soil food web, continues even when plant inputs are reduced or absent. Decomposition of SOM is strongly influenced by soil temperature and moisture and higher temperature and moisture levels generally stimulate decomposition (Wiesmeier et al., 2019). The altered microclimatic conditions below solar panels may reduce the SOM losses by slowing down decomposition when soil temperature and/or moisture are reduced (Lambert et al., 2021). Still, a severe reduction in plant biomass, however, is likely to decrease SOM over time until a new steady SOM level is reached.

Changes in SOM content occur slowly and are difficult to detect (Smith et al., 2020). However, soil biota respond more rapidly to changes in land use and soil conditions and may therefore serve as early indicators for changes in SOM dynamics (Fierer et al., 2021; Rutgers et al., 2009). Whether there will be an increase or decrease of SOM content between and below the panels over time will also depend on previous land-use (Cesar et al., 2022; Lal et al., 2021; Wiesmeier et al., 2019). Solar parks are often managed as (extensive) grasslands. On former arable fields, the construction of solar parks may result in a build-up of SOM due to a change from annual to perennial biodiverse grassland vegetation (Guo & Gifford, 2002). When constructed on former (agricultural) grasslands, the future SOM level may depend on the vegetation productivity of the new sward. Regardless of the total carbon balance of a solar park, the spatial distribution of SOM and soil properties is expected to change over time in response to the impacts of the solar panels (Moscatelli et al., 2022). Due to the scarcity of studies, it remains unclear how and to what extent solar parks impact plant productivity and soil health, though this knowledge is critical for informing the design of solar parks that support healthy soil ecosystems during their lifespan and beyond.

This study aimed to assess the influence of solar parks on plant productivity, SOM and microbial community biomass and composition beneath versus between solar panels. It also sought to identify the influence of key characteristics, such as light and the microclimate, park age, soil type and previous land use on plant and soil responses to solar parks across the Netherlands. It was hypothesised that 1) plant biomass is lower below the panels compared to between the panels, but the magnitude of decrease depends on the level of shading below panels, 2) microbial biomass and litter decomposition rates below the panels are lower due to a lower carbon input and lower average temperatures and that 3) SOM stocks below the panels are lower than between the panels due to a larger reduction of plant carbon inputs relative to the reduction in decomposition rates.

2 | MATERIAL AND METHODS

2.1 | Solar park sampling sites

This study was conducted in 17 solar parks across The Netherlands (see Figure S1 for the location of the sites). The solar parks differed in spatial configuration of the panels, park size, age and previous land use (Table 1). The solar panels in each solar park were mounted in fixed arrays - i.e., no tracking systems were used. A total of 14 of the solar parks were built on land that was either managed as agricultural grassland or arable land, while 3 were built on fallow land. One solar park (HIL) had its topsoil removed, which was placed along the edge of the solar park. The vegetation within the solar parks was managed

TABLE 1 Overview of solar park characteristics. The locations of the park IDs can be found in Figure S1. Vegetation management frequency: number of times the vegetation was mown or grazed by sheep. NA: frequency unknown; EW: east–west; S: south. Hmax and Hmin: height of top and bottom edge of solar arrays, respectively. The array width in EW-orientated solar parks is the width of one array; gap: gap between two solar arrays.

Park ID	Year of construction	Previous land use	Size (ha)	Vegetation management	Vegetation management frequency (# per year)	Orientation	Hmax (cm)	Hmin (cm)	Array width (cm)	Gap (cm)	Soil type
AIJ	2021	Grassland	5	Mowing	2–3	EW	200	105	1,032	190	Sand
ALM	2018	Grassland	2	Mowing	1	S	180	60	400	500	Clay
DBK	2018	Arable/grassland rotation	3	Mowing	2	S	150	40	470	700	Sand
DUI	2019	Wasteland	1	Mowing	3	S	152	50	400	240	Clay
GOE	2020	Arable	4	Mowing	3	S	140	60	307	100	Clay
HAR	2020	Grassland	33	Mowing	2	S	150	60	330	205	Clay
HIL	2018	Arable	16	Mowing	2	S	250	95	590	280	Sand
HOU	2021	Grassland	17	Mowing	5	S	195	75	500	230	Clay
HVZ	2018	Grassland	14	Grazing	2–3	S	250	90	550	300	Sand
HWG	2021	Grassland	7	Mowing	NA	S	150	60	565	350	Clay
MAR	2018	Grassland	8	Grazing	Year-round	S	210	62	774	250	Sand
ROO	2021	Arable	33	Grazing	3	EW	240	90	750	250	Sandy loam
SOL	2021	Arable	12	Grazing	2–3	S	240	90	630	250	Sand
TEG	2021	Wasteland	6	Grazing	Year-round	S	244	80	630	500	Sandy loam
THO	2021	Arable	17	Mowing	2	S	145	65	405	260	Clay
WBG	2020	Wasteland	3	Grazing	Year-round	EW	150	45	1,200	105	Clay
ZUN	2021	Arable	14	Mowing	NA	S	150	60	560	150	Sand

as grassland and was either mown or grazed by sheep. The area below the panels was not mown unless vegetation tended to grow above the panels. Herbicides were not used in any of the solar parks.

2.2 | Soil sampling protocol

A standardised sampling protocol was used across all solar parks. Within each solar park, four spatial blocks were randomly selected for sampling, though areas that were too wet were excluded in some parks. Within each block, soil and vegetation samples were taken at two positions referred to as 'below' and 'gap', under and between the panels, respectively (Figure 1). To assess plant productivity and to place soil temperature and humidity TMS-4 dataloggers (TOMST) (Wild et al., 2019), a smaller plot within each block was excluded from grazing or mowing. In May 2022, soil cores (1.5 cm diameter, 0–20 cm) were collected per block at 10 sampling points (outside the vegetation plot) parallel to the panel rows and were subsequently mixed to form composite samples for each position (Figure 1). Immediately after sampling, the soil was stored in cooling boxes and then stored for a maximum of 2 weeks at 4°C. The fresh soil was sieved at 5 mm and subsamples were taken for hot water extractable carbon (HWC) and stored at 4°C, and phospholipid fatty acid (PLFA) analysis, which was stored at −20°C. The remaining soil was air-dried at 40°C for 72 h, sieved further through a 2 mm mesh, and stored dry for further analysis. Adjacent to the vegetation plots, two bulk density (BD) cores (5 cm diameter, 100 cm^3) were extracted, one at a depth of 7.5 cm and one at 17.5 cm and combined to calculate an average BD for the top 20 cm (Figure 1). BD samples were oven-dried at 105°C, weighed and the BD was calculated as the ratio of the soil dry weight over the volume of the cylinder.

2.3 | Soil chemical and biological parameters

Hot water extractable carbon (HWC) was determined using the protocol by Ghani et al. (2003). Briefly, 4 g of fresh soil and 30 ml of deionised water were added to a 50 ml polypropylene centrifuge tube and shaken for 30 min at 150 rpm. The samples were subsequently centrifuged for 20 min at 3000 rpm. The supernatant, containing water-soluble carbon, was discarded. A total of 30 ml of deionised water was again added to the samples, vortexed to suspend the pellet and heated at 80°C for 16 h. After heating, the samples were vortexed to suspend the pellet and centrifuged for 20 min at 3000 rpm. The supernatant was filtered through a 0.45 μm DOC-free filter and the total carbon of the filtered solution was determined on a SAN++ analyser (Skalar Analytical B.V., Breda, the Netherlands).

Total soil carbon (C) and nitrogen (N) were measured on dried, sieved and finely ground (ball-milled) soil on a CN828 analyser (LECO Corporation; Saint Joseph, Michigan USA). Soil C and N stocks were calculated as the product of C and N concentration and the bulk density. The concentration of SOM was determined by loss of ignition

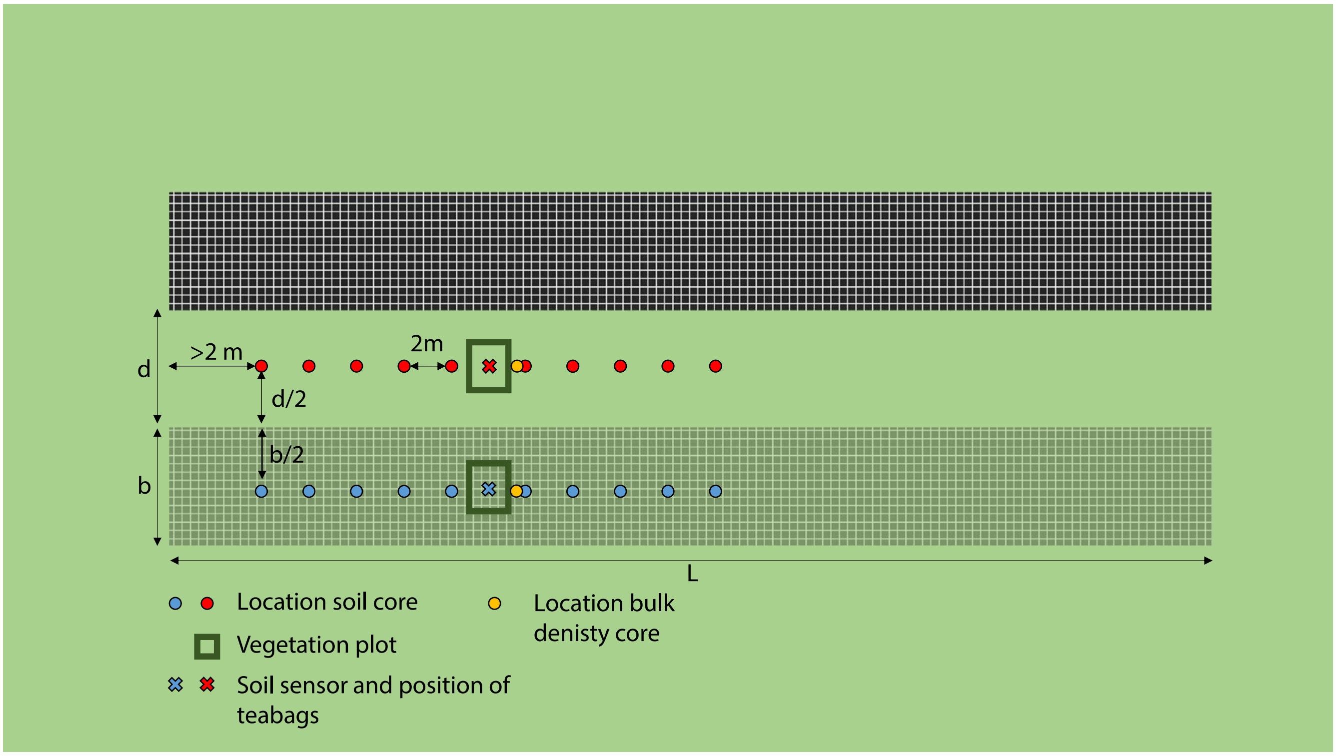

FIGURE 1 Schematic sampling design for soil and vegetation samples for one block; per solar park four of these blocks were sampled. L: length solar arrays; d: width gap between array rows; b: width solar arrays. Red dots: sampling locations in the gap between panels; blue dots: sampling locations below the panels. Dark and pale rectangles: solar arrays.

(LOI) as the weight loss of oven-dried (105°C for 24 h) soil after burning the soil at 550°C for 3 h (Hoogsteen et al., 2015).

The levels of NH_4^+, NO_3^- and total soluble nitrogen (N_{ts}) in soil were quantified by soil extraction with 0.01 M $CaCl_2$. Briefly, approximately 3 g of air-dried sieved soil was added to a 50 ml polypropylene centrifuge tube together with 30 ml of 0.01 M $CaCl_2$ solution and shaken for 2 h at 150 rpm. After shaking, the pH was measured for each sample. The samples were then centrifuged for 10 min at 3000 rpm and the supernatant was filtered through a 0.45 μm filter and NH_4^+, NO_3^- and N_{ts} of the filtered solution were measured by a SAN++ analyser (Skalar Analytical B.V., Breda, the Netherlands).

To quantify the soil microbial biomass of bacteria and saprotrophic fungi, PLFAs were extracted from 2 g of freeze-dried soil. PLFAs were extracted based on established methods (Frostegard & Baath, 1996; Hedlund, 2002). PLFAs 15:0, 16:1ω9 and 18:1ω7 were used as general bacterial biomarkers, i15:0, a15:0, i16:0, i17:0 and a17:0 were used as biomarkers for gram-positive bacteria, cy17:0 and cy19:0 for gram-negative bacteria, 10Me16:0 10Me17:0 and 10Me18:0 for actinobacteria and 18:2ω6c for saprotrophic fungi. The total amount of bacterial PLFAs was calculated as the sum of general bacteria, gram-positive and gram-negative bacteria. The fungal-to-bacterial ratio was calculated as the ratio of PLFA 18:2ω6c to total bacterial PLFAs.

2.4 | Vegetation characteristics and root colonisation by AMF

Within the plots with temporal exclusion of grazing and mowing, the vegetation was mown in April 2022 below the panels and the gap in order to measure the regrowth. The aboveground biomass was then harvested in July (harvest 1) and in October 2022 (harvest 2). Aboveground biomass was collected from 50 × 50 cm squares at the centre of both the gap and the below-panel area (Figure 1). The aboveground vegetation was clipped to a height of 2 cm, dried for 72 h at 70°C and weighed. The dry samples were ball-milled, and C and N content was measured by a Flash*Smart* Elemental Analyser (Thermo Fisher Scientific Inc., Waltham MA, USA). Additionally, for harvest 2, root samples were taken with a 10 cm diameter, 0–20 cm depth corer in the centre of each 50 × 50 cm area where aboveground biomass was harvested. Roots were washed, weighed fresh and subsampled for arbuscular mycorrhizal fungi (AMF) colonisation. The remaining roots were dried for 72 h at 70°C and then weighed. Some samples that were taken below panels lacked sufficient root material for subsampling and in these cases, all the root material was used for AMF colonisation and the dry biomass was estimated using the fresh weight of those samples and the average water content of the samples that had enough root material for both fresh and dry weight quantification. Root-to-shoot ratios were calculated to estimate the above- and belowground plant biomass partitioning. AMF colonisation was visualised by staining AMF inside the roots with the ink and vinegar method (Vierheilig et al., 1998). Stained root fragments of each root sample were placed in five lines on a microscope glass slide. Per microscope slide, 100 observations were made under the microscope with 40 × 10 magnification and scored for the absence or presence of AMF in the roots (McGonigle et al., 1990). Root colonisation by AMF was expressed as % root length colonisation.

2.5 | Decomposition rate

The Tea Bag Index (TBI) (Keuskamp et al., 2013) was used to assess potential litter decomposition rates. Tea bags, one containing green tea (EAN 8722700 05552 5) and one rooibos (EAN 8711327 5,143 48), were buried at 8 cm depth at each position below and between the panels in May 2022. Before burying, the bags were weighed. After approximately 90 days, the bags were collected and stored at 4°C before drying them for 48 h at 70°C. After drying, soil and root particles were carefully removed, and the bags were weighed again. The stabilisation factor S and decomposition factor k were calculated as follows: $S = 1 - (ag/Hg)$, where ag is the fraction of decomposed green tea (1 – final weight green tea/initial weight green tea) and Hg the hydrolysable fraction of green tea (0.842); $k = \ln(ar/(Wt - [1-ar]))/t$, where ar is the predicted labile fraction of red tea (Hr*[1-S]) with Hr the hydrolysable fraction of rooibos tea (0.552), Wt the fraction of remaining rooibos tea (final weight rooibos tea – initial weight rooibos tea) and t time in days.

2.6 | Microclimate

To measure the effect of solar panels on the microclimate TMS-4 dataloggers (TOMST) (Wild et al., 2019) were placed between and below the panels within the vegetation plots in three of the four blocks in each solar park (Figure 1). Air (+ 15 cm), surface (0 cm), soil (8 cm depth) temperature and soil moisture (0–15 cm depth) were measured every 15 min between 01-05-2022 and 01-11-2022. The TMS soil moisture signals were transformed to volumetric soil moisture and were calibrated per soil type (sand and clay) with gravimetric soil moisture values from soil samples. The raw temperature and moisture data were converted to daily means, and daily temperature extremes (Tmin and Tmax). Temperature and soil moisture seasonality were calculated as the standard deviation × 100 (https://www.worldclim.org/data/bioclim.html). Growing degree days (GDDs) were calculated from the daily mean air temperature values.

2.7 | Irradiance modelling

To estimate the level of shading caused by the panels, the BIGEYE model was used to simulate incoming solar irradiance across space (Barros et al., 2022). BIGEYE is a model that is designed to simulate the electrical output of solar panels, but as an intermediate step calculates the ground irradiance which is used here as a proxy for light intensity reaching the vegetation within the solar park. The incoming irradiance was modelled every 10 minutes at a spatial resolution of

10 cm × 10 cm and then integrated for the growing season (March until October) (Cesar et al., 2022). The irradiance (in W m^{-2}) for each position (gap and below) within each solar park was converted to a % of the total incoming irradiance.

2.8 | Statistical analysis

Statistical analyses were performed in R version 4.1.0 (R Core Team, 2021) and RStudio version 2024.4.2.764 (Posit Team, 2024). Linear mixed-effects models using the *lme* function from the nlme package (Pinheiro et al., 2022) were performed to assess the effect of solar panels on plant biomass production and soil parameters with position (between vs below panels) as a fixed factor, and plot and site (solar park) as random factors. One-way ANOVA tests were performed on these models to test significance. Normal distribution of residuals and homogeneity of variance were tested visually using *QQplots* and by plotting the residuals vs the fitted values. When assumptions were not met, the data were transformed (either log or sqrt) to meet the assumptions. To test the effect of microclimatic variables (light, air and soil temperature and soil moisture) we performed multiple linear regressions using linear mixed-effects models (see above). To account for the effect of panels, panel position was included as a random factor and nested within the plot and site. Before running the models, the variables were scaled and collinear variables with a *rho* > 0.7 were removed from the analysis. Automated backward selection was performed with the *dredge* function from the MuMIn package (Bartoń, 2022). An ANOVA test was then performed on the model with the best fit.

3 | RESULTS

3.1 | Microclimate and solar irradiation

There were large variations in temperature and soil moisture between parks, sometimes with contrasting patterns, especially for soil moisture (Figures S2-S5). Nevertheless, across all parks, the mean monthly soil temperature was significantly higher in the gap between the solar panels than below the panels from May through July (on average 1.11, 1.24 and 1.03°C higher for May, June and July, respectively) and lower in October (0.59°C lower) ($p < 0.0001$ for May, June, July and October; Figure 2a; Table S2). Furthermore, the daily minimum and maximum soil temperature in these months in late spring and early summer were also higher for the gap. The differences in mean surface and air temperature for the months May, June and July were much smaller (< 0.50°C difference), while still being significant for surface temperature but not significant for air temperature. Conversely, the surface and air temperature in the gap showed larger extremes than below the panels, with lower minimum temperatures and higher maximum temperatures with up to 3.18°C higher maximum air temperatures in July in the gap (Figure 2b,c).

Soil moisture varied less over time below the solar panels than in the gap (Figure 2d) and was higher during July and August. The soil in the area in the gap between the panels became very dry in these months, in line with the meteorological recordings for these months in 2022 (Royal Netherlands Meteorological Institute [KNMI]). In autumn this pattern of soil moisture was reversed, with higher soil moisture levels in the soil in between the panels compared to below the panels as of mid-September (Figure 2d).

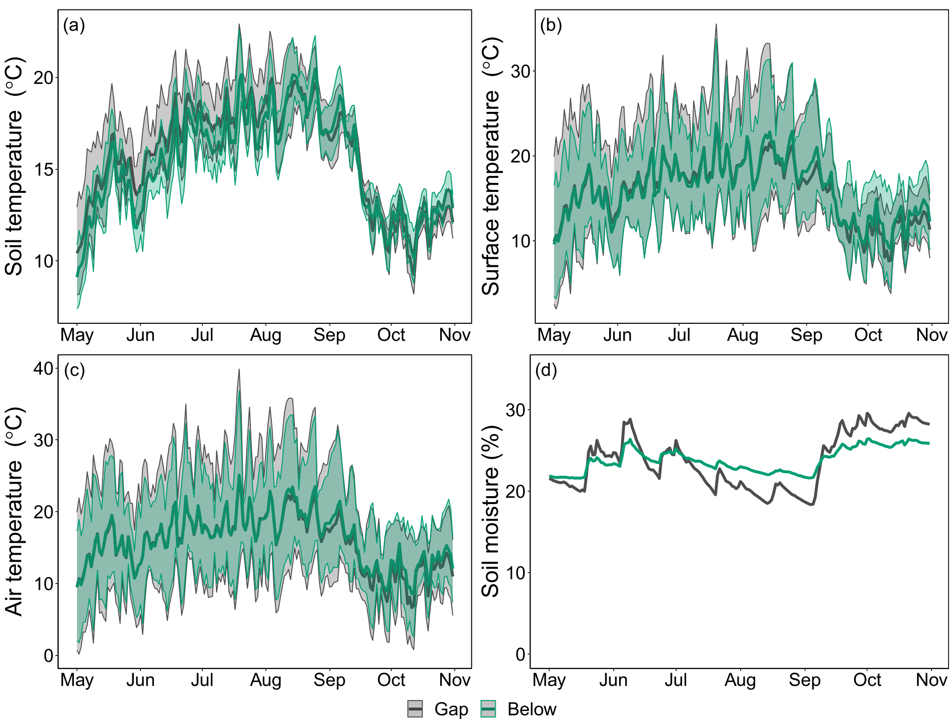

FIGURE 2 Temperature at different locations (soil surface (a), air (+ 15 cm) (b) and topsoil (8 cm depth) (c) temperature) and soil moisture (0–15 cm depth) (d) in between (grey, gap) and under (green, below) the solar panels across all solar parks (n = 17). Data from the sensors were converted to daily values for both positions (n = 3 sensors per position per solar park). Average daily values are shown by the lines. Daily minimum and maximum temperatures are shown as ribbons around the lines to show daily variation. Dark green indicates an overlap in temperature between and below panels and light green indicates when the temperature below the panels is higher or lower than in the gap.

The average light levels for the plots below panels ranged from 1 to 10% of the open field radiation, while light levels in the gap between the panels ranged from 30 to 90% (Figure S6). This large variation in light availability in the gap between sites was primarily determined by the distance between solar arrays and to a lesser extent by the width of the solar arrays.

3.2 | Vegetation biomass and AMF colonisation

Plant above- and belowground biomass was significantly reduced under the panels and was on average 80% lower below than between the panels for both harvests and across all parks ($p < 0.0001$) (Figure 3a,b). Additionally, the C:N ratio of plants was significantly lower below panels than between panels, with an average C:N ratio of 13 below compared to 28 in between the panels ($p < 0.0001$; Figure 3c). AMF colonisation was significantly reduced below panels ($p < 0.0001$; Figure 3d). The average aboveground biomass produced during the growing period April–October ranged from 1.9 to 8 Mg ha^{-1} between the panels and from 0.03 to 3.43 Mg ha^{-1} below the panels (Figure 3a). In two solar parks (ROO and WBG), vegetation below panels was almost absent. In general, the vegetation below panels was patchy and spots of bare soil without vegetation were common. Vegetation management did not have a significant effect on vegetation biomass ($p > 0.05$).

The variation in the configuration of solar panels across solar parks created a large variation in light availability for plant growth. Light levels were significantly and positively related to vegetation productivity ($p < 0.0001$) (Figure 4). GDD correlated negatively with plant aboveground biomass production ($p < 0.0001$; Table S3, Figure S7), while soil moisture seasonality correlated positively ($p = 0.0028$; Table S3, Figure S8). We found no significant difference in the root-to-shoot (R:S) ratio ($p > 0.05$). Soil NO_3^- and N_{ts} were significantly higher below the panels compared to the gap ($p < 0.0001$; Table S4).

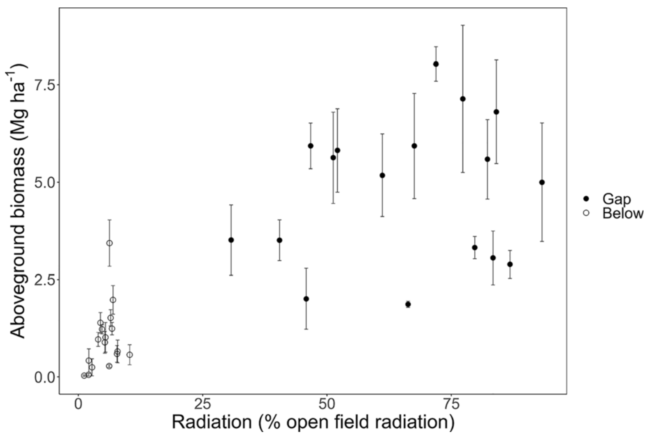

FIGURE 4 Aboveground biomass in relation to light availability to the vegetation as a % of open field radiation. Dots represent the mean of the cumulative biomass for harvest 1 and 2 combined for each position and each site (n = 17). Error bars depict the standard error (n = 4).

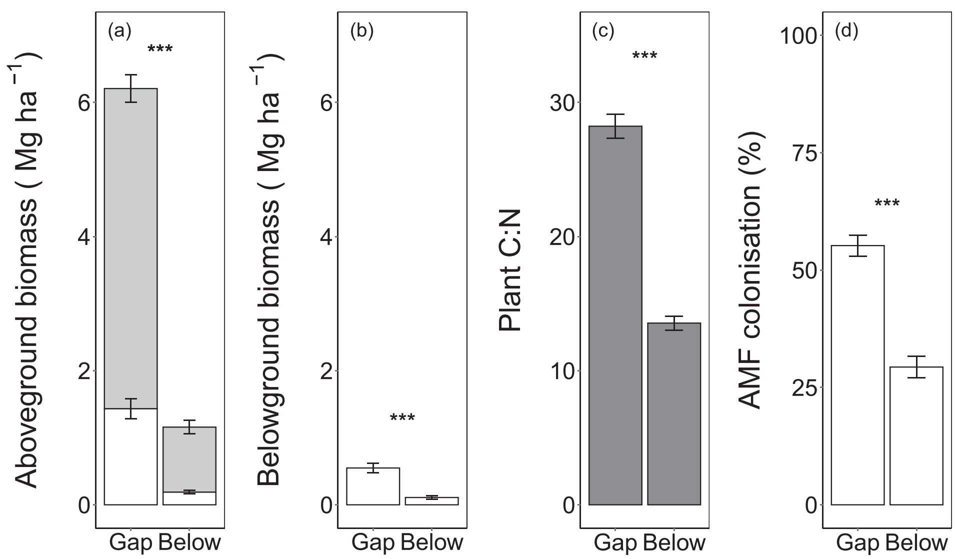

FIGURE 3 *Aboveground (a) and belowground (b) plant biomass, plant C:N ratio of the shoots (c) and arbuscular mycorrhizal fungi (AMF) colonisation (d) of the vegetation grown under (below) or in between (gap) the solar panels across all solar parks (n = 17). Error bars depict the standard error (n = 68 for aboveground biomass and plant C:N ratio, n = 44 for belowground biomass). Aboveground biomass was harvested twice, in July (panel (a) light grey part of the bar) and October 2022 (panel (a) white part of the bar). Belowground biomass (b) and AMF colonisation (d) (in white) were only collected in October. Plant aboveground C:N ratio depicted (in dark grey) is the mean for both harvests. Significant differences are indicated by * ($p < 0.05$), ** ($p < 0.001$), *** ($p < 0.0001$).*

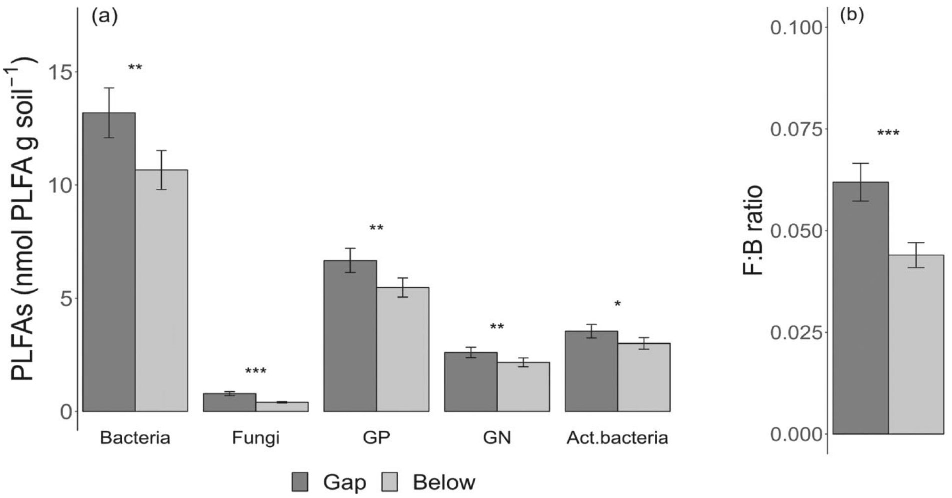

FIGURE 5 Phospholipid fatty acids (PLFA) levels (nmol PLFA soil $^{-1}$) (a) and the fungal to bacterial ratio (b) for the different microbial groups and for each position across all solar parks (n = 17). GP = gram-positive bacteria; GN = gram-negative bacteria. Significant differences are indicated by * ($p < 0.05$), ** ($p < 0.001$), *** ($p < 0.0001$).

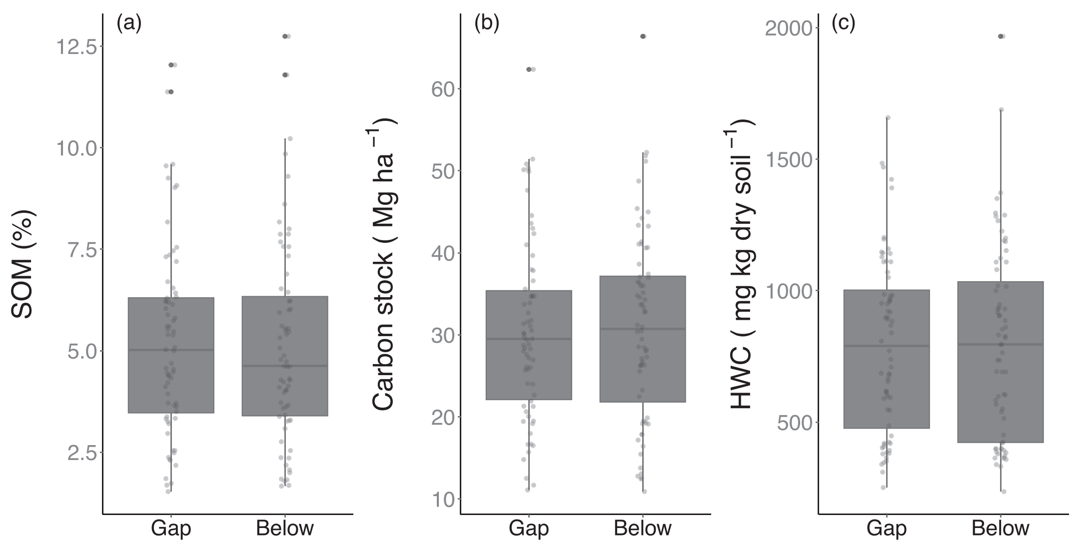

FIGURE 6 Soil organic matter (SOM) (a), soil carbon stock (b) and hot water extractable carbon (HWC) (c) between (gap) and under (below) the solar panels across all solar parks (n = 17).

3.3 | Soil microbial biomass and litter decomposition rate

The biomass of both fungal and bacterial PLFAs was lower in the soil below the panels compared to in between the panels (Figure 5a; $p < 0.0001$ for fungi; $p = 0.001$ for total bacteria). Additionally, the biomass of the bacterial subgroups actinobacteria, gram-positive and gram-negative bacteria separately was also lower below the panels (Figure 5a; $p = 0.0175$ for actinobacteria; $p = 0.0029$ for gram-positive bacteria; $p = 0.0081$ for gram-negative bacteria). Furthermore, F:B ratio was significantly lower below panels due to the stronger decrease for fungi ($p < 0.0001$; Figure 5b).

Despite the lower soil microbial biomass and lower average soil temperature below the panels as compared to in between the panels (May–July) litter decomposition rates were not significantly different based on the TBI decomposition rate *k* (0.017 on average) and stabilisation factor *S* (0.31 on average) ($p > 0.05$) (Table S5).

3.4 | SOM and soil carbon

There were no differences in any of the organic carbon pools in the soil (SOM, carbon stock and HWC) between and below panels ($p > 0.05$) (Figure 6). The solar parks varied in time of construction, but all were built relatively recently, the oldest existing for four years at the time of sampling (Table 1). The age of construction, soil type, previous land use and solar park design (EW vs S) had no significant effect on SOM ($p > 0.05$). Furthermore, the panels had no effect on the soil C:N ratio. Although the difference was small, in parks on clay soil the soil bulk density was significantly lower below panels than between panels ($p = 0.0059$). This was not the case in parks on sandy soils (Table S5).

4 | DISCUSSION

The presented results demonstrate that solar parks influence vegetation productivity, microclimate and soil microbial abundances across the Netherlands. In the following sections, we examine the mechanisms behind these changes and discuss their implications for long-term carbon storage and soil health.

4.1 | Microclimate

Climate is a key driver of SOM dynamics and influences both carbon inputs through plant growth and carbon outputs through SOM decomposition (Wiesmeier et al., 2019). Therefore, by changing the microclimate, solar parks may directly influence these processes. The results of this study show that on average temperature was lower below the panels during summer and daytime, with a more pronounced effect on mean soil temperature compared to air temperature (Figure 2) (Zheng et al., 2023). Conversely, the average temperature was higher below the panels during nighttime and winter (Armstrong et al., 2016; Yue et al., 2021; Zheng et al., 2023). These results can be explained by the fact that solar panels block the direct incoming (shortwave) radiation, resulting in a cooling effect below panels during the day. On the other hand, by trapping longwave radiation emitted from the soil, solar panels increase average nighttime temperatures below the panels (Armstrong et al., 2016; Barron-Gafford et al., 2016; Zheng et al., 2023).

Nighttime warming may have contrasting effects on the vegetation: on the one hand, it can increase leaf respiration thereby reducing plant growth, on the other hand, it may also increase photosynthesis during the subsequent day through overcompensation mechanisms (Peng et al., 2013; Wan et al., 2009). However, for overcompensation to occur, plants need sufficient energy to renew carbohydrate losses from nighttime respiration. As the vegetation in the studied solar parks is limited by light and thereby energy to photosynthesise (Figure 4), such photosynthetic overcompensation is unlikely to occur. Therefore, the increased nighttime temperatures may result in net carbon losses without compensatory gains during the day.

Soil moisture was generally higher below the panels during summer and lower during autumn and winter across all parks (Figure 2d). However, there was considerable variation in soil moisture patterns between solar parks, where some parks experienced flooded conditions below and between panels (Figure S6). Furthermore, soil moisture below the panels varied less throughout the year compared to the soil in the gap between the panels. These patterns are likely driven by reduced temperature and lower plant productivity below the panels, contributing to lower evapotranspiration rates. Additionally, previous studies have shown that wind speed is reduced, and wind direction altered in solar parks, especially below the solar panels, which could potentially slow down evapotranspiration (Adeh et al., 2018; Armstrong et al., 2016; Zheng et al., 2023).

Conversely, incoming rainfall is likely to be reduced below panels although Armstrong et al. (2016) observed higher water inputs under the panels due to rainwater being funnelled along the supporting solar panel frame. The resulting soil moisture below panels is likely context-dependent and may depend on the setup of the solar arrays, soil type and groundwater table and vegetation cover. For example, in some solar parks, there was a clear spatial heterogeneity in moisture below the panels, with driplines where rainwater accumulated below the separation between two panels, and very dry soil beside those driplines. It must be noted that the sensors were never placed inside the driplines, and as such we did not measure this spatial heterogeneity in soil moisture. In other solar parks, this spatial heterogeneity below the panels was much less apparent, particularly in parks with wetter conditions overall, such as those experiencing periods of flooding. The change in microclimatic conditions, and particularly the observed periods of extended flooding, could result in anaerobic conditions. These conditions typically favour increased emissions of greenhouse gases such as methane or nitrous oxide, and may have implications for net greenhouse gas balances of solar parks (Zhang et al., 2023), highlighting the need for further research.

4.2 | Vegetation

Plant above- and belowground biomass below the panels was reduced for all solar parks. On average, the above- and belowground biomass below the panels was reduced by 80% compared to the biomass between the panels (Figure 3), although this reduction varied from 50% to almost 100% and was strongly correlated with light availability. As light becomes more limiting for plant growth, other factors such as soil fertility become less important. Consequently, the range of vegetation biomass between sites was larger in the gap than below the panels, which could explain the large range in the reduced biomass below the panels. These results are in line with other studies that assessed the impact of solar panels on plant biomass (Armstrong et al., 2016; Li et al., 2023; Moscatelli et al., 2022; Sturchio et al., 2022), or vegetation cover (Knegt et al., 2021; Lambert et al., 2023; Uldrijan et al., 2022). However, some studies report an increase in plant biomass below the panels (Adeh et al., 2018), or only minimal decreases (Sturchio, Kannenberg, & Knapp, 2024). Liu et al. (2023) found a decrease in biomass under the panels with reduced precipitation, but an increase with increased precipitation. These contrasting results of the different studies could be explained by a difference in climate. In semi-arid and arid climates where plants are water-limited, solar parks may have a beneficial effect on vegetation by reducing water loss from evapotranspiration (Adeh et al., 2018; Knapp & Sturchio, 2024). Conversely, in temperate regions plants are light (energy) limited, explaining the negative impact of solar panels on the vegetation below (Adeh et al., 2018). These results are in line with what was found in the present study, where light availability had a strong positive influence on vegetation biomass (Figure 4).

Conversely, GDD was negatively correlated with the vegetation biomass (Figure S7). This is contrary to what was expected, as GDD generally positively influences plant growth (Soltani & Sinclair, 2012). A potential explanation is that during the growing season, especially after the first harvest, there was a period of drought, and this could have influenced the regrowth of the vegetation and explained the observed negative relationship with GDD and vegetation productivity. Furthermore, Sturchio, Kannenberg, Pinkowitz, and Knapp (2024) found that the timing of direct sunlight throughout the day is important in maintaining photosynthesis in a semi-arid grassland. In their study, Sturchio, Kannenberg, Pinkowitz, and Knapp (2024) found that the vegetation receiving direct sunlight in the morning performed better than the vegetation receiving direct sunlight in the afternoon, which was related to drought stress impeding plant growth despite high solar energy availability.

Even though shading reduces solar energy availability plants may still grow well under moderate shade levels (Pang et al., 2019; Semchenko et al., 2012). The experiments by Pang et al. (2019) and Semchenko et al. (2012) were performed under controlled conditions, where stresses other than light were minimised. Under field conditions, plants are likely to experience multiple stresses at once, both biotic and abiotic, that influence their ability to tolerate shade (Valladares et al., 2016). Therefore, under suboptimal conditions, plants may need more than the minimum amount of light to survive. In addition, shade-tolerant plant species may be better adapted to grow below the panels (Valladares & Niinemets, 2008). Plant species distribution has indeed been shown to change towards more shade-tolerant species below panels (Armstrong et al., 2016; Lambert et al., 2023). The presence of shade-tolerant species may be constrained by the limited dispersal of these species into the solar parks (Ehrlén & Eriksson, 2000). Sowing of shade-tolerant plant species could therefore be a potential solution in reducing the impact of solar panels on vegetation productivity. If sowing is done, selecting native species adapted to the local environment should be favoured to avoid the introduction of non-native or invasive species.

In addition, the soil NO_3^- and dissolved organic nitrogen concentrations were much higher below the solar panels compared to in between, suggesting that the vegetation below the panels was not limited by nitrogen, which is often a limited nutrient in grasslands (LeBauer & Treseder, 2008). This observation is further corroborated by the lower plant C:N ratio below the panels (Figure 3). The high NO_3^- levels below the panels and reduced absolute N uptake by the plants increase the risk of nitrate leaching to groundwater and N_2O emissions to the atmosphere. As N_2O is a potent GHG gas such emissions can counteract the contribution of solar parks to offset GHG emissions (Zhang et al., 2023). While nitrogen is likely not a limiting factor, growth may still be constrained by phosphorus and micronutrient availability, as their uptake is often facilitated by AMF (Smith & Read, 2008). In this study, AMF colonisation was significantly lower beneath the panels, likely due to the limited energy available for symbiosis. This decline in AMF colonisation could thus further amplify the negative effects of shading on plant growth.

In this study, we have shown that solar panels significantly reduce plant growth beneath them, with potential consequences for ecosystem health and functioning. Identifying solar park design and management strategies that balance renewable energy production and environmental health is crucial. As mentioned before, sowing shade-tolerant plant species could be a potential solution. However, since even shade-tolerant species require sufficient light to grow, increased light availability below the panels is essential. One straightforward option to increase light availability is to decrease the density of panels per unit of land, although this would also decrease electricity production. Alternative options include using tracking systems that follow the sun, which have been shown to increase light below panels (Sturchio et al., 2022), or by using semi-transparent panels that allow for some sunlight to penetrate through the panels (Cesar & Van Aken, 2025). However, these options will likely increase the costs of developing solar parks and may require additional governmental aid to facilitate the development of ecological sound solar parks. More research is needed to guide solar park development towards optimal designs that identify the 'sweet spots' between maximising energy production and maintaining environmental health.

4.3 | Soil

Contrary to what was expected, the levels of SOM, HWC and carbon stocks did not differ significantly between and under the panels in this study (Figure 6). At the time of sampling, the age of the solar parks ranged from 1 to 4 years. Even with very little or no carbon inputs to the soil, this timeframe may have been too short to detect differences in SOM (Smith et al., 2020). Similar findings in carbon or SOM content are reported at 2–3 years after construction in the UK (Armstrong et al., 2016), five years after construction in China (Li et al., 2023) and seven years after construction in Colorado, USA (Choi et al., 2020). Moscatelli et al. (2022) found that seven years after solar panel installation, soil organic carbon (SOC) concentration was higher in the gaps than beneath the panels or in an adjacent arable field. Since the previous land use was arable farming - the same as the adjacent field - this suggests SOC in the gaps increased over time due to conversion to grassland (Guo & Gifford, 2002), rather than simply decreasing beneath the panels. Furthermore, Lambert et al. (2023) found a higher soil carbon concentration outside the solar panels, but no difference between the gap and under the panels in 10 solar parks in southern France, although the age of these solar parks was not given.

SOM dynamics depend on both carbon inputs from plants and carbon outputs from SOM decomposition. Although no changes in SOM were apparent at the time of this study, the reductions in plant and microbial biomass may serve as an early indicator that SOM is expected to decrease below panels (Fierer et al., 2021; Rutgers et al., 2009). In the soil below the panels, fungi were more strongly reduced than bacteria, up to almost 50% reduction in biomass (Figure 5), in line with previous studies (Lambert et al., 2023). The lower microbial biomass, in combination with lower average temperatures below the panels may be associated with decreasing SOM decomposition which would reduce the rate of soil carbon loss. However, based on the decomposition rates from the TeaBagIndex (TBI) we did not observe different decomposition rates between and below the panels, contrary to what was hypothesised. While the TBI is a sensitive method to detect differences in decomposition rates across different biomes (Keuskamp et al., 2013), the different microclimatic conditions between and below panels may not have been large enough to detect potential differences in decomposition rates. For example, other studies found lower in situ soil respiration below the panels (Armstrong et al., 2016; Lambert et al., 2023). However, total soil respiration (or ecosystem respiration) also includes respiration from plant roots. A reduction in plant biomass below panels may therefore lead to a reduction in measured soil respiration, although this does not necessarily mean a change in SOM decomposition (Kuzyakov & Gavrichkova, 2010). It is therefore unclear whether SOM decomposition is significantly altered below the panels, which warrants further research on soil respiration across different plant biomass levels, including in the absence of plants. In the long term, SOM content is expected to decrease below the panels, which may diminish the associated ecosystem functions such as carbon storage, water retention and nutrient cycling (Hoffland et al., 2020), which are important for agricultural production.

4.4 | Limitations and future directions

This study covered a diverse range of solar parks, capturing realistic variations in soil types, previous land uses and array configurations. While this diversity strengthens the generalisability of our findings, it also presents challenges for drawing specific conclusions about optimal solar park design. While we found that light reduction resulted in the reduction of plant growth below panels, we could not determine threshold values of light availability for sustained plant growth that is sufficient to maintain soil health. For example, the light patterns of solar parks used in this study did not allow for precise sampling of vegetation across a gradient of light availability levels due to the fast transition between 'light' (i.e. the gap) and 'dark' (i.e. below the panels) (Figure S6), future research should aim to employ experimental setups that can systematically determine minimum light requirements below panels.

An important consideration for the evaluation of solar parks is their net effect on greenhouse gas emissions and net carbon balance. While the presented results suggest carbon stocks to reduce over time, due to the often severe reduction in plant growth and maintained decomposition of SOM, we did not measure significant differences in carbon pools below and between panels, potentially due to the young age of the parks in this study. Long-term monitoring and sampling of older sites should be done to verify this assumption. Furthermore, the presented results can only provide a snapshot view of the potentially maintained decomposition of SOM, however, we did not measure soil respiration and greenhouse gas emissions in this study.

5 | CONCLUSIONS

Solar parks are an important measure to mitigate climate change by producing low-carbon energy. At the same time, solar parks change soil–plant interactions that can counteract its climate mitigation effect due to carbon and nitrogen losses to the atmosphere. There is a need to investigate how to design solar parks without environmental burden. In this study, we have shown that, despite differences in solar park setup, plant growth and the soil microbial biomass, two key drivers in soil organic matter dynamics, were greatly reduced below solar panels across the 17 studied solar parks in The Netherlands. Light availability was the most important factor explaining the changes in plant growth. While we could not detect any changes in SOM content due to solar panels, it is likely that SOM levels below the panels will decrease over time given the large reduction in plant growth. It is therefore crucial to design solar parks in such a way that these impacts are minimised. Mitigating these impacts, however, is likely to result in trade-off between electricity production and may require creative solutions. For example, using tracking systems (Sturchio et al., 2022) utilising semi-transparent solar panels (Cesar & Van Aken, 2025) or the use of vertical bifacial panels could be explored.

AUTHOR CONTRIBUTIONS

Design of the research: LS, GDD, RdG; **Performance of the research:** LS; **data analysis**: LS, AE; **data collection**: LS, BVA; **data interpretation:** LS, GDD, RdG, AE, BVA; **writing the manuscript:** LS, GDD, RdG, AE.

ACKNOWLEDGEMENTS

This study is part of the project EcoCertified Solar Parks. It was funded with Topsector Energy grant MOOI-22004 from Rijksdienst voor Ondernemend Nederland, and funds from Rijkswaterstaat, the Provinces of Friesland, Drenthe, Flevoland, Overijssel, Gelderland, Utrecht, Noord-Holland and Limburg and the Natuur & Milieufederaties. We would like to thank the solar park developers that financially supported this project and granted permission to access the solar parks. We thank Jaap Bloem for his advice on the experimental design and help with the interpretation of the data, especially the PLFA and HWC data. We would like to thank Karen Krijgsveld for her constructive feedback on the manuscript and Sebastiaan Forouzan Fard for facilitating access to the solar parks. Thanks to Willeke van Tintelen, Henk Martens and Tamás Salánki for their help in the lab, and Henk van Roekel, Gerrit Huisman, Dafydd Timmerman, Erne Blondeau, Zhongchen Yang, Felipe Bonini da Luz, Bert Scholten and Bastiaan Meinders for their help in the field. We would like to thank Kay Cesar and Teun Burgers for their contribution on the development and validation of the BIGEYE model. Finally, we thank the three anonymous reviewers for their constructive feedback.

CONFLICT OF INTEREST STATEMENT

The authors declare that they have no known competing financial interests or personal relationships that could have appeared to influence the work reported in this paper.

DATA AVAILABILITY STATEMENT

The data that support the findings of this study are openly available in fig share at https://doi.org/10.6084/m9.figshare.28388246.

ORCID

Luuk Scholten https://orcid.org/0009-0004-0703-0728
Ron G. M. de Goede https://orcid.org/0000-0002-9786-5187
Anna Edlinger https://orcid.org/0000-0003-3538-2371
Bas B. Van Aken https://orcid.org/0000-0003-1532-2216
Gerlinde B. De Deyn https://orcid.org/0000-0003-4823-6912

REFERENCES

Abraham, E. M., Kyriazopoulos, A. P., Parissi, Z. M., Kostopoulou, P., Karatassiou, M., Anjalanidou, K., & Katsouta, C. (2014). Growth, dry matter production, phenotypic plasticity, and nutritive value of three natural populations of Dactylis glomerata L. under various shading treatments. *Agroforestry Systems*, *88*, 287–299. https://doi.org/10.1007/s10457-014-9682-9

Adeh, E. H., Selker, J. S., & Higgins, C. W. (2018). Remarkable agrivoltaic influence on soil moisture, micrometeorology and water-use efficiency. *PLoS ONE*, *13*, 1–15.

Adhikari, K., & Hartemink, A. E. (2016). Linking soils to ecosystem services - a global review. *Geoderma*, *262*, 101–111. https://doi.org/10.1016/j.geoderma.2015.08.009

Armstrong, A., Ostle, N. J., & Whitaker, J. (2016). Solar park microclimate and vegetation management effects on grassland carbon cycling. *Environmental Research Letters*, *11*, 1–11.

Armstrong, A., Waldron, S., Whitaker, J., & Ostle, N. J. (2014). Wind farm and solar park effects on plant-soil carbon cycling: Uncertain impacts of changes in ground-level microclimate. *Global Change Biology*, *20*, 1699–1706. https://doi.org/10.1111/gcb.12437

Barron-Gafford, G. A., Minor, R. L., Allen, N. A., Cronin, A. D., Brooks, A. E., & Pavao-Zuckerman, M. A. (2016). The photovoltaic heat island effect: Larger solar power plants increase local temperatures. *Scientific Reports*, *6*, 1–7.

Barros, E. G. D., Van Aken, B. B., Burgers, A. R., Slooff-Hoek, L. H., & Fonseca, R. M. (2022). Multi-objective optimization of solar park design under climatic uncertainty. *Solar Energy*, *231*, 958–969. https://doi.org/10.1016/j.solener.2021.12.026

Bartoń, K. (2022). MuMIn: Multi-model inference. R package version 1.46.0. https://CRAN.R-project.org/package=MuMIn

Bennun, L., van Bochove, J., Ng, C., Fletcher, C., Wilson, D., Phair, N., & Carbone, G. (2021). *Mitigating biodiversity impacts associated with solar and wind energy development: Guidelines for project developers*. IUCN, International Union for Conservation of Nature.

Bugera, S., & Tillema, M. (2023). Kadaster onderzoeksrapport naar zonneparken in Nederland. (At: https://www.kadaster.nl/documents/d/kadaster.nl/kadaster-onderzoeksrapport-naar-zonneparken-in-nederland-1. Accessed: 19/2/2025).

Bünemann, E. K., Bongiorno, G., Bai, Z., Creamer, R. E., De Deyn, G., de Goede, R., Fleskens, L., Geissen, V., Kuyper, T. W., Mäder, P., Pulleman, M., Sukkel, W., van Groenigen, J. W., & Brussaard, L. (2018). Soil quality – A critical review. *Soil Biology and Biochemistry*, *120*, 105–125. https://doi.org/10.1016/j.soilbio.2018.01.030

Carvalho, F., Treasure, L., Robinson, S. J. B., Blaydes, H., Exley, G., Hayes, R., Howell, B., Keith, A., Montag, H., Parker, G., Sharp, S. P., Witten, C., & Armstrong, A. (2023). Towards a standardized protocol to assess natural capital and ecosystem services in solar parks. *Ecological Solutions and Evidence*, *4*, e12210. https://doi.org/10.1002/2688–8319.12210

Cesar, I., & Van Aken, B. B. (2025). Evaluation method and module design for cost-effective compliance with irradiance guidelines to maintain soil quality in solar parks. *EPJ Photovoltaics*, *16*, 13. https://doi.org/10.1051/epjpv/2025003

Cesar, K., van Aken, B., Scholten, L., de Goede, R., & Schotman, A. (2022). Nieuwe ontwerptoets verankert bodemkwaliteit in zonneparken. *Bodem*, *32*, 34–36.

Choi, C. S., Cagle, A. E., Macknick, J., Bloom, D. E., Caplan, J. S., & Ravi, S. (2020). Effects of revegetation on soil physical and chemical properties in solar photovoltaic infrastructure. *Frontiers in Environmental Science*, *8*, 1–10.

Creamer, R. E., Barel, J. M., Bongiorno, G., & Zwetsloot, M. J. (2022). The life of soils: Integrating the who and how of multifunctionality. *Soil Biology and Biochemistry*, *166*, 108561. https://doi.org/10.1016/j.soilbio.2022.108561

Ehrlén, J., & Eriksson, O. (2000). Dispersal limitation and patch occupancy in forest herbs. *Ecology*, *81*, 1667–1674. https://doi.org/10.1890/0012–9658(2000)081[1667:DLAPOI]2.0.CO;2

Fierer, N., Wood, S. A., & Bueno de Mesquita, C. P. (2021). How microbes can, and cannot, be used to assess soil health. *Soil Biology and Biochemistry*, *153*, 108111. https://doi.org/10.1016/j.soilbio.2020.108111

Frostegard, A., & Baath, E. (1996). The use of phospholipid fatty acid analysis to estimate bacterial and fungal biomass in soil. *Biology and Fertility of Soils*, *22*, 59–65.

Ghani, A., Dexter, M., & Perrott, K. W. (2003). Hot-water extractable carbon in soils: A sensitive measurement for determining impacts of fertilisation, grazing and cultivation. *Soil Biology and Biochemistry*, *35*, 1231–1243. https://doi.org/10.1016/S0038-0717(03)00186-X

Guo, L. B., & Gifford, R. M. (2002). Soil carbon stocks and land use change: A meta analysis. *Global Change Biology*, *8*, 345–360. https://doi.org/10.1046/j.1354–1013.2002.00486.x

Hedlund, K. (2002). Soil microbial community structure in relation to vegetation management on former agricultural land. *Soil Biology & Biochemistry*, *34*, 1299–1307. https://doi.org/10.1016/S0038-0717(02)00073–1

Hernandez, R. R., Armstrong, A., Burney, J., Ryan, G., Moore-O'Leary, K., Diédhiou, I., Grodsky, S. M., Saul-Gershenz, L., Davis, R., Macknick, J., Mulvaney, D., Heath, G. A., Easter, S. B., Hoffacker, M. K., Allen, M. F., & Kammen, D. M. (2019). Techno–ecological synergies of solar energy for global sustainability. *Nature Sustainability*, *2*, 560–568.

Hernandez, R. R., Easter, S. B., Murphy-Mariscal, M. L., Maestre, F. T., Tavassoli, M., Allen, E. B., Barrows, C. W., Belnap, J., Ochoa-Hueso, R., Ravi, S., & Allen, M. F. (2014). Environmental impacts of utility-scale solar energy. *Renewable and Sustainable Energy Reviews*, *29*, 766–779. https://doi.org/10.1016/j.rser.2013.08.041

Hoffland, E., Kuyper, T. W., Comans, R. N. J., & Creamer, R. E. (2020). Eco-functionality of organic matter in soils. *Plant and Soil*, *455*, 1–22. https://doi.org/10.1007/s11104-020-04651-9

Hoogsteen, M. J. J., Lantinga, E. A., Bakker, E. J., Groot, J. C. J., & Tittonell, P. A. (2015). Estimating soil organic carbon through loss on ignition: Effects of ignition conditions and structural water loss. *European Journal of Soil Science*, *66*, 320–328. https://doi.org/10.1111/ejss.12224

Janzen, H. H., van Groenigen, K. J., Powlson, D. S., Schwinghamer, T., & van Groenigen, J. W. (2022). Photosynthetic limits on carbon sequestration in croplands. *Geoderma*, *416*, 115810. https://doi.org/10.1016/j.geoderma.2022.115810

Keuskamp, J. A., Dingemans, B. J. J., Lehtinen, T., Sarneel, J. M., & Hefting, M. M. (2013). Tea bag index: A novel approach to collect uniform decomposition data across ecosystems. *Methods in Ecology and Evolution*, *4*, 1070–1075. https://doi.org/10.1111/2041-210X.12097

Knapp, A. K., & Sturchio, M. A. (2024). Ecovoltaics in an increasingly water-limited world: An ecological perspective. *One Earth*, *7*, 1705–1712. https://doi.org/10.1016/j.oneear.2024.09.003

Knegt, C. G. M., van Wijngaanden, K., Verweij, P. A., & Soons, M. B. (2021). De effecten van zonneparken op vegetatie. *Landschap*, *2*, 81–89.

Kuzyakov, Y., & Gavrichkova, O. (2010). REVIEW: Time lag between photosynthesis and carbon dioxide efflux from soil: A review of mechanisms and controls. *Global Change Biology*, *16*, 3386–3406. https://doi.org/10.1111/j.1365-2486.2010.02179.x

Lal, R., Monger, C., Nave, L., & Smith, P. (2021). The role of soil in regulation of climate. *Philosophical Transactions of the Royal Society B: Biological Sciences*, *376*, 20210084.

Lambert, Q., Bischoff, A., Cueff, S., Cluchier, A., & Gros, R. (2021). Effects of solar park construction and solar panels on soil quality, microclimate, CO2 effluxes, and vegetation under a Mediterranean climate. *Land Degradation & Development*, *32*, 5190–5202.

Lambert, Q., Bischoff, A., Enea, M., & Gros, R. (2023). Photovoltaic power stations: An opportunity to promote European semi-natural grasslands? *Frontiers in Environmental Science*, *11*, 1137845.

LeBauer, D. S., & Treseder, K. K. (2008). Nitrogen limitation of net primary productivity in terrestrial ecosystems is globally distributed. *Ecology*, *89*, 371–379. https://doi.org/10.1890/06-2057.1

Li, C., Liu, J., Bao, J., Wu, T., & Chai, B. (2023). Effect of light heterogeneity caused by photovoltaic panels on the plant–soil–microbial system in solar park. *Land*, *12*, 367.

Liu, Z., Peng, T., Ma, S., Qi, C., Song, Y., Zhang, C., Li, K., Gao, N., Pu, M., Wang, X., Bi, Y., & Na, X. (2023). Potential benefits and risks of solar photovoltaic power plants on arid and semi-arid ecosystems: An assessment of soil microbial and plant communities. *Frontiers in Microbiology*, *14*, 1190650. https://doi.org/10.3389/fmicb.2023.1190650

Makaronidou, M. (2020). *Assessment on the local climate effects of solar photovoltaic parks*. Thesis. Lancaster University.

Masson-Delmotte, V., Zhai, P., Pirani, A., Connors, S. L., Péan, C., Berger, S., Caud, N., Chen, Y., Goldfarb, L., Gomis, M. I., Huang, M., Leitzell, K., Lonnoy, E., Matthews, J. B. R., Maycock, T. K., Waterfield, T., Yelekçi, O., Yu, R., & Zhou, B. (2021). IPCC, 2021: Summary for Policymakers. In *Climate change 2021: The physical science basis. Contribution of working group I to the sixth assessment report of the intergovernmental panel on climate change*. Cambridge University Press. In Press

McGonigle, T. P., Miller, M. H., Evans, D. G., Fairchild, G. L., & Swan, J. A. (1990). A new method which gives an objective measure of colonization of roots by vesicular—Arbuscular mycorrhizal fungi. *New Phytologist*, *115*, 495–501. https://doi.org/10.1111/j.1469-8137.1990.tb00476.x

Moscatelli, M. C., Marabottini, R., Massaccesi, L., & Marinari, S. (2022). Soil properties changes after seven years of ground mounted photovoltaic panels in Central Italy coastal area. *Geoderma Regional*, *29*, e00500. https://doi.org/10.1016/j.geodrs.2022.e00500

Pang, K., Van Sambeek, J. W., Navarrete-Tindall, N. E., Lin, C. H., Jose, S., & Garrett, H. E. (2019). Responses of legumes and grasses to non-, moderate, and dense shade in Missouri, USA. I. Forage yield and its species-level plasticity. *Agroforestry Systems*, *93*, 11–24. https://doi.org/10.1007/s10457-017-0067-8

Peng, S., Piao, S., Ciais, P., Myneni, R. B., Chen, A., Chevallier, F., Dolman, A. J., Janssens, I. A., Peñuelas, J., Zhang, G., Vicca, S., Wan, S., Wang, S., & Zeng, H. (2013). Asymmetric effects of daytime and night-time warming on northern hemisphere vegetation. *Nature*, *501*, 88–92. https://doi.org/10.1038/nature12434

Pierson, E. A., Mack, R. N., & Black, R. A. (1990). The effect of shading on photosynthesis, growth, and regrowth following defoliation for Bromus tectorum. *Oecologia*, *84*, 534–543. https://doi.org/10.1007/BF00328171

Pinheiro, J., Bates, D., and R Core Team. (2022). nlme: Linear and nonlinear mixed effects models. R package version 3.1-161. https://CRAN.R-project.org/package=nlme

Poorter, H., Niinemets, Ü., Ntagkas, N., Siebenkäs, A., Mäenpää, M., Matsubara, S., & Pons, T. L. (2019). A meta-analysis of plant responses to light intensity for 70 traits ranging from molecules to whole plant performance. *New Phytologist*, *223*, 1073–1105. https://doi.org/10.1111/nph.15754

Posit Team. (2024). RStudio: Integrated development environment for R. Posit Software, PBC. http://www.posit.co/

R Core Team. (2021). R: A language and environment for statistical computing. R Foundation for Statistical Computing. https://www.R-project.org/

Rutgers, M., Schouten, A. J., Bloem, J., Van Eekeren, N., De Goede, R. G. M., Jagers Op Akkerhuis, G. A. J. M., Van Der Wal, A., Mulder, C., Brussaard, L., & Breure, A. M. (2009). Biological measurements in a nationwide soil monitoring network. *European Journal of Soil Science*, *60*, 820–832.

Semchenko, M., Lepik, M., Götzenberger, L., & Zobel, K. (2012). Positive effect of shade on plant growth: Amelioration of stress or active regulation of growth rate? *Journal of Ecology*, *100*, 459–466. https://doi.org/10.1111/j.1365-2745.2011.01936.x

Smith, P., Soussana, J. F., Angers, D., Schipper, L., Chenu, C., Rasse, D. P., Batjes, N. H., van Egmond, F., McNeill, S., Kuhnert, M., Arias-Navarro, C., Olesen, J. E., Chirinda, N., Fornara, D., Wollenberg, E., Álvaro-Fuentes, J., Sanz-Cobena, A., & Klumpp, K. (2020). How to measure, report and verify soil carbon change to realize the potential of soil carbon sequestration for atmospheric greenhouse gas removal. *Global Change Biology*, *26*, 219–241. https://doi.org/10.1111/gcb.14815

Smith, S., & Read, D. (2008). Chapter 5: Mineral nutrition, heavy metal accumulation and water relations of VA mycorrhizal plants. *Mycorrhizal Symbiosis*, *3*, 126–160.

Soltani, A., & Sinclair, T. R. (2012). Chapter 6 Phenology-Temperature. In *Modeling physiology of crop development, growth and yield* (pp. 55–72). CABi.

Sturchio, M. A., Kannenberg, S. A., & Knapp, A. K. (2024). Agrivoltaic arrays can maintain semi-arid grassland productivity and extend the seasonality of forage quality. *Applied Energy*, *356*, 122418. https://doi.org/10.1016/j.apenergy.2023.122418

Sturchio, M. A., Kannenberg, S. A., Pinkowitz, T. A., & Knapp, A. K. (2024). Solar arrays create novel environments that uniquely alter plant responses. *Plants, People, Planet*, *6*, 1522–1533. https://doi.org/10.1002/ppp3.10554

Sturchio, M. A., & Knapp, A. K. (2023). Ecovoltaic principles for a more sustainable, ecologically informed solar energy future. *Nature Ecology and Evolution*, *7*, 1746–1749. https://doi.org/10.1038/s41559-023-02174-x

Sturchio, M. A., Macknick, J. E., Barron-Gafford, G. A., Chen, A., Alderfer, C., Condon, K., Hajek, O. L., Miller, B., Pauletto, B., Siggers, J. A., Slette, I. J., & Knapp, A. K. (2022). Grassland productivity responds unexpectedly to dynamic light and soil water environments induced by photovoltaic arrays. *Ecosphere*, *13*(12), e4334. https://doi.org/10.1002/ecs2.4334

Uldrijan, D., Černý, M., & Winkler, J. (2022). Solar Park: Opportunity or threat for vegetation and ecosystem. *Journal of Ecological Engineering*, *23*, 1–10. https://doi.org/10.12911/22998993/153456

Valladares, F., Laanisto, L., Niinemets, Ü., & Zavala, M. A. (2016). Shedding light on shade: Ecological perspectives of understorey plant life. *Plant Ecology and Diversity*, *9*, 237–251. https://doi.org/10.1080/17550874.2016.1210262

Valladares, F., & Niinemets, Ü. (2008). Shade tolerance, a key plant feature of complex nature and consequences. *Annual Review of Ecology*, *Evolution, and Systematics*, *39*, 237–257. https://doi.org/10.1146/annurev.ecolsys.39.110707.173506

van Hooff, W., Sinke, W., Post, R., Janson, B., Kolkman, M., & Kooi, K. (2019). Hernieuwbare elektriciteitsopwekking op land en de gebouwde omgeving (MMIP 2). (At: https://www.topsectorenergie.nl/sites/default/files/uploads/MMIP/MMIP2-Hernieuwbareelektriciteitsopwekkingoplandendegebouwdeomgeving.pdf.).

Vierheilig, H., Coughlan, A. P., Wyss, U., & Piché, Y. (1998). Ink and vinegar, a simple staining technique for arbuscular-mycorrhizal fungi. *Applied and Environmental Microbiology*, *64*, 5004–5007. https://doi.org/10.1128/AEM.64.12.5004–5007.1998

Wan, S., Xia, J., Liu, W., & Niu, S. (2009). Photosynthetic overcompensation under nocturnal warming enhances grassland carbon sequestration. *Ecology*, *90*, 2700–2710. https://doi.org/10.1890/08–2026.1

Wiesmeier, M., Urbanski, L., Hobley, E., Lang, B., von Lützow, M., Marin-Spiotta, E., van Wesemael, B., Rabot, E., Ließ, M., Garcia-Franco, N., Wollschläger, U., Vogel, H. J., & Kögel-Knabner, I. (2019). Soil organic carbon storage as a key function of soils - a review of drivers and indicators at various scales. *Geoderma*, *333*, 149–162. https://doi.org/10.1016/j.geoderma.2018.07.026

Wild, J., Kopecký, M., Macek, M., Šanda, M., Jankovec, J., & Haase, T. (2019). Climate at ecologically relevant scales: A new temperature and soil moisture logger for long-term microclimate measurement. *Agricultural and Forest Meteorology*, *268*, 40–47. https://doi.org/10.1016/j.agrformet.2018.12.018

Yue, S., Guo, M., Zou, P., Wu, W., & Zhou, X. (2021). Effects of photovoltaic panels on soil temperature and moisture in desert areas. *Environmental Science and Pollution Research*, *28*, 17506–17518. https://doi.org/10.1007/s11356-020-11742-8

Zhang, B., Zhang, R., Li, Y., Wang, S., & Xing, F. (2023). Ignoring the effects of photovoltaic Array deployment on greenhouse gas emissions may Lead to overestimation of the contribution of photovoltaic power generation to greenhouse gas reduction. *Environmental Science and Technology*, *57*, 4241–4252. https://doi.org/10.1021/acs.est.3c00479

Zheng, J., Luo, Y., Chang, R., & Gao, X. (2023). An observational study on the microclimate and soil thermal regimes under solar photovoltaic arrays. *Solar Energy*, *266*, 112159. https://doi.org/10.1016/j.solener.2023.112159

SUPPORTING INFORMATION

Additional supporting information can be found online in the Supporting Information section at the end of this article.

How to cite this article: Scholten, L., de Goede, R. G. M., Edlinger, A., Van Aken, B. B., & De Deyn, G. B. (2025). Sharing the light, impact of solar parks on plant productivity, soil microbes and soil organic matter. *Plants, People, Planet*, 1–14. https://doi.org/10.1002/ppp3.70011